Routes to Heavy Fermions

Peter Fulde

Max–Planck-Institut für Physik komplexer Systeme

Bayreuther Str. 40, D-01187 Dresden, Germany

Abstract

Heavy-fermion excitations require the presence of a low-energy scale in the system. In recent years it has become clear that these scales can result from rather different physical processes. The Kondo effect is one of them, certainly the one most studied. We describe and discuss in addition to Kondo lattices two other sources of heavy quasiparticles: the Zeeman route to heavy fermions which applies to $Nd_{2-x}Ce_xCuO_4$ ($0.1 \leq x \leq 0.2$) and a scenario of nearly half-filled Hubbard chains which is related to the semimetal Yb_4As_3. It is suggested that these are not the only processes leading to heavy-fermion behaviour.

1 Introduction

The investigation of heavy-fermion systems with heavy-quasiparticle excitations has developed into a new branch of low-temperature physics. Recent reviews have been given of theoretical (Lee et al., 1986; Fulde et al., 1988; Schlottmann, 1984; Zwicknagl, 1993; Norman and Koelling, 1993; Kasuya, 1993; Hewson, 1993) and experimental (Stewart, 1984; Ott, 1988; Grewe and Steglich, 1991; Wachter, 1994) developments in this field. In most cases these compounds contain Ce, Yb, U or Np as one of their constituents, implying that $4f$ or $5f$ electrons are involved. Examples are the metals $CeAl_3$, $CeCu_2Si_2$, $CeRu_2Si_2$, $CeCu_6$, $YbCu_2Si_2$, UBe_{13}, UPt_3, and $NpBe_{13}$. But also the electron-doped cuprate $Nd_{2-x}Ce_xCuO_4$ shows heavy-fermion behaviour (Brugger et al., 1993) in the range of $0.1 \leq x \leq 0.2$. Heavy-fermion excitations have also been found in semimetals like Yb_4As_3, Sm_3Se_4 or in some of the Ce and Yb monopnictides and even in insulators like YbB_{12} or SmB_6 (see, for example, Proc., 1995).

We speak of heavy-fermion behaviour when a system meets the following conditions: (a) The low temperature specific heat $C = \gamma T$ has a coefficient γ of order 1 $\mathrm{Jmol^{-1}K^{-2}}$, rather than 1 $\mathrm{mJmol^{-1}K^{-2}}$ as, e.g., found for sodium metal; (b) the Pauli susceptibility χ_s is similarly enhanced as γ; (c) the ratio $R = \pi^2 k_B^2 \chi_s / (3\mu_{\mathrm{eff}}^2 \gamma)$

(Sommerfeld–Wilson ratio) is of order unity. Here μ_{eff} is the effective magnetic moment of the quasiparticles. Both quantities γ and χ_s are proportional to the quasiparticle density of states at the Fermi level $N^*(0)$. The latter is proportional to m^*, i.e., the effective mass of the fermionic excitations. Large values of γ and χ_s can therefore be interpreted by ascribing a large m^* to the quasiparticles. When R is calculated, the density of states $N^*(0)$ drops out. For free electrons $R = 1$, while in the presence of quasiparticle interactions $R = (1 + F_0^a)^{-1}$. The Landau parameter F_0^a relates to the interactions and enters χ_s. When conditions (a)–(c) are met, we may assume a one-to-one correspondence between the quasiparticle excitations of the complex system and those of a free electron gas, provided we use the effective mass m^* and, in the case of semimetals or insulators, the effective charge e^*, instead of the corresponding bare quantities.

Heavy-fermion behaviour requires the presence of a low-energy scale in the system. Usually, that scale is characterized by a temperature T^*. As the temperature of the system increases to values above T^*, the quasiparticles lose their heavy-mass character. The specific heat levels off, and the susceptibility changes from Pauli- to Curie-like behaviour. With increasing temperature the rare-earth or actinide ions behave more and more like ions with well-localized f electrons.

One key problem is to understand the physical origin of the low-energy scales. Until few years ago, it was commonly believed that the Kondo effect is the sole source of heavy-fermion behaviour. The physics associated with the Kondo effect is extensively described in a monograph by Hewson (1993) and a number of reviews (Lee at al., 1986; Fulde et al., 1988; Schlottmann, 1984; Zwicknagl, 1993; Norman and Koelling, 1993; Kasuya, 1993). However, more recently it has been found that heavy quasiparticles may result from rather different physical effects. In all cases a lattice of $4f$ (or $5f$) ions is involved. In metallic systems it is coupled to conduction electrons. In that case the conduction electrons can be either weakly correlated like in $CeAl_3$, or they can be strongly correlated like in the high-T_c cuprates. In the latter case the correlations are perhaps not as strong as those of the f electrons, but they may influence substantially the physical properties of the system. This situation is encountered, e.g., in $Nd_{2-x}Ce_xCuO_4$ and it will be shown later that here the Zeeman effect is responsible for the formation of heavy fermions. In a semimetal like Yb_4As_3, the heavy quasiparticles result from the $4f$ electron system itself, i.e., without having a coupling to conduction electrons crucially contributing. Thus, instead of having one single physical origin, heavy fermions may have a variety of effects responsible for their existence.

Obviously, the low-lying excitations characterizing heavy-fermion systems involve predominantly spin degrees of freedom. Direct evidence is given by the amount of entropy associated with the excess specific heat. The latter is associated with an entropy of order $S \simeq k_B \ln \nu_f$ per f site, where ν_f denotes the degeneracy

of the crystal-field ground state of the atomic f shell. It is pretty safe to state that in all likelihood yet unknown mechanisms will add to the presently known ones. In the following, a discussion is given of the three routes to heavy-fermion behaviour just outlined.

2 Kondo lattices

The essence of the single-site Kondo effect is the formation of a singlet ground-state due to a weak hybridization of the incomplete $4f$ shell with the conduction electrons. A specific form of the singlet wavefunction is obtained by starting from the Anderson impurity Hamiltonian

$$\begin{aligned} H &= \sum_{km} \epsilon(k) c^+_{km} c_{km} + \epsilon_f \sum_m n^f_m + \frac{U}{2} \sum_{m \neq m'} n^f_m n^f_{m'} + \\ &+ \sum_{km} V(k)(f^+_m c_{km} + c^+_{km} f_m) + \tilde{H}_0. \end{aligned} \tag{1}$$

Here f^+_m denotes the creation operator of an f electron in state m of the lowest J multiplet and $n^f_m = f^+_m f_m$. The f-orbital energy is ϵ_f and U is the $f - f$ Coulomb repulsion. The c^+_{km} create conduction electrons with momentum $|\mathbf{k}| = k$ and the three quantum numbers $\ell = 3$, J and m. The hybridization between the f and conduction electrons is given by the matrix element $V(k)$. Finally, $\tilde{H}_0$ contains all those degrees of freedom of the conduction electrons which do not couple to the impurity. The following ansatz for the singlet ground-state wave function is due to Varma and Yafet (1976).

$$|\psi_0\rangle = A\Big(1 + \frac{1}{\sqrt{\nu_f}} \sum_{km} \alpha(k) f^+_m c_{km}\Big) |\phi_0\rangle \tag{2}$$

where $|\phi_0\rangle$ represents the Fermi sea of the conduction electrons. The ansatz (2) is closely related to the one suggested by Yoshida (1966; see also Yoshida and Yoshimori, 1973) for the ground state of the Kondo Hamiltonian. The variational parameters A and $A\alpha(k)$ are obtained by minimizing the energy. The energy E_0 of $|\psi_0\rangle$ is always lower than the one of the multiplet $|\psi_m\rangle = f^+_m |\phi_0\rangle$. The difference ϵ is found to be

$$\epsilon = -D \exp[-|\epsilon_f| / (\nu_f N(0) V^2)] \tag{3}$$

and denotes the energy gain due to the formation of the singlet. Here D is half of the bandwidth of the conduction electrons and $N(0)$ is their density of states per spin direction at the Fermi energy. It is customary to associate with this energy gain a temperature T_K, i.e., the Kondo temperature. The singlet-triplet

excitation energy is often of the order of a few meV only, and provides a low-energy scale. When a lattice of f ions is considered like, e.g., $CeAl_3$ the Anderson lattice Hamiltonian replaces Eq. (1). The energy scale $k_B T_K$ is replaced here by $k_B T^*$ which takes into account modifications in the presence of the lattice, i.e., due to interactions between different f sites. The energy gain due to singlet formation competes here with the one due to the RKKY interaction when the f sites are in a magnetic state (Doniach, 1971, 1987). In the limit of small hybridization V the RKKY interaction energy always wins out because it is proportional to V^4 while the singlet-formation energy depends exponentially on V, see Eq. (3), and therefore is smaller. This seems to be the case in systems like $CeAl_2$, $CePb_3$ and $NpBe_{13}$ which become antiferromagnets at low temperatures.

In addition to T^* there exists another characteristic temperature $T_{\rm coh} < T^*$ below which the local singlet-triplet excitations lock together and form coherent quasiparticles with large effective masses. The details of this coupling are not yet understood, but de Haas–van Alphen measurements demonstrate convincingly that the f electrons behave like delocalized electrons. At the Fermi surface they show strong anisotropies in the effective mass. It is somewhat surprising that one can calculate the Fermi surface of a heavy-electron system and determine the anisotropic masses with one adjustable parameter only. This is achieved by renormalized band-structure calculations (Zwicknagl, 1993, 1990; Razafimandimby et al., 1984; d'Ambrumenil and Fulde, 1985; Sticht et al., 1986; Strange and Newns, 1986; Zwicknagl et al., 1990). Thereby the effective potential seen by a quasiparticle is described by energy-dependent phase shifts $\eta_\ell^A(\epsilon)$ of the different atoms A. The index ℓ refers to the different angular momentum channels.

In the following we consider $CeRu_2Si_2$ as an example (Zwicknagl, 1993, 1990; Zwicknagl et al., 1990). The essential point is to use for the phase shifts the ones computed within the local-density approximation (LDA) to density functional theory, with the exception of the $\ell = 3$ phase shift of the Ce ion. This approximation neglects the coupling of conduction electrons to different configurations of the $4f$ or $5f$ shell with *fixed* f electron number. [The mass enhancement of the conduction electrons of Pr metal falls into that category. It results from the virtual transitions between different crystal-field eigenstates of the $4f^2$ system caused by the coupling between conduction and $4f$ electrons (Fulde and Jensen, 1983; see also White and Fulde, 1981)]. Thus, only the $\eta_{\ell=3}^{\rm Ce}(\epsilon)$ phase shift remains undetermined. According to Hund's rules the ground-state multiplet of the $4f^2$ configuration of Ce is $J = 5/2$ with the $J = 7/2$ multiplet being much higher in energy. Therefore, we may set $\eta_{J=7/2}^{\rm Ce}(\epsilon_F) = 0$. Of the $J = 5/2$ multiplet, only the Kramers-degenerate crystal-field ground state is considered, because it is the only state occupied at low temperatures. Let τ denote the degeneracy index of that ground state. Only the phase shift $\eta_\tau^{\rm Ce}(\epsilon_F)$ among the different $\ell = 3$ channels differs then from zero. It

must contain the strong correlations of the $4f$ electrons and is unknown. In the spirit of Landau's Fermi liquid theory we expand this unknown function around the Fermi energy and write

$$\eta_\tau^{\mathrm{Ce}}(\epsilon) = \eta_\tau^{\mathrm{Ce}}(\epsilon_F + a(\epsilon - \epsilon_F) + O((\epsilon - \epsilon_F)^2). \tag{4}$$

Of the two parameters one, i.e., $\eta_\tau^{\mathrm{Ce}}(\epsilon_F)$ is fixed by requiring that the number of $4f$ electrons $n_f = 1$. According to Friedel's sum rule this implies $\eta_\tau^{\mathrm{Cu}}(\epsilon_F) = \frac{\pi}{2}$. The remaining parameter a fixes the slope of the phase shift at ϵ_F. The latter determines the density of states and hence the effective mass. We set $a = (k_B T^*)^{-1}$ and determine T^* by requiring that the linear specific heat coefficient γ calculated from the resulting quasiparticle dispersions agrees with the experimental one. The different computational steps are summarized in Fig. 1. Calculations of this form have explained and partially predicted (Zwicknagl, 1993, 1990; Zwicknagl et al., 1990) the large mass anisotropies in $CeRu_2Si_2$ (Lonzarich, 1988). For more details on renormalized band theory we refer to comprehensive reviews which are available (Zwicknagl, 1993; Norman and Koelling, 1993).

When the temperature increases beyond T_{coh} the excitations lose their coherence properties and the problem reduces to that of independent impurities. In that regime the specific heat contains large contributions from the incoherent part of the f electron excitations. The noncrossing approximation (NCA) is a valuable tool for treating the coupled $4f$ and conduction electrons in that temperature regime (Aoki et al., 1993; Keiter and Kimball, 1971; Kojima et al., 1984). It leads to a system of coupled equations of the form

$$\begin{aligned} \Sigma_0(z) &= \frac{\Gamma}{\pi} \sum_m \int_{-\infty}^{+\infty} d\zeta \, \rho_m(\zeta) K_+(z - \zeta) \\ \Sigma_m(z) &= \frac{\Gamma}{\pi} \int_{-\infty}^{+\infty} d\zeta \, \rho_0(\zeta) K_-(z - \zeta). \end{aligned} \tag{5}$$

Here $\Gamma = \pi N(0) V^2$ and $K_\pm(z)$ are defined by

$$K_\pm(z) = \frac{1}{N(0)} \int_{-\infty}^{+\infty} d\epsilon \, \frac{N(\pm\epsilon) f(\epsilon)}{z + \epsilon} \tag{6}$$

where $f(\epsilon)$ is the Fermi energy and $N(\epsilon)$ is the energy-dependent conduction-electron density of states. The function $\Sigma_\alpha(z)$ and $\rho_\alpha(z)$ $(\alpha = 0; m)$ are related to each other through

$$\begin{aligned} \rho_\alpha(z) &= -\frac{1}{\pi} \mathrm{Im}\{R_\alpha(z)\} \\ R_\alpha(z) &= \frac{1}{z - \epsilon_\alpha - \Sigma_\alpha(z)} \end{aligned} \tag{7}$$

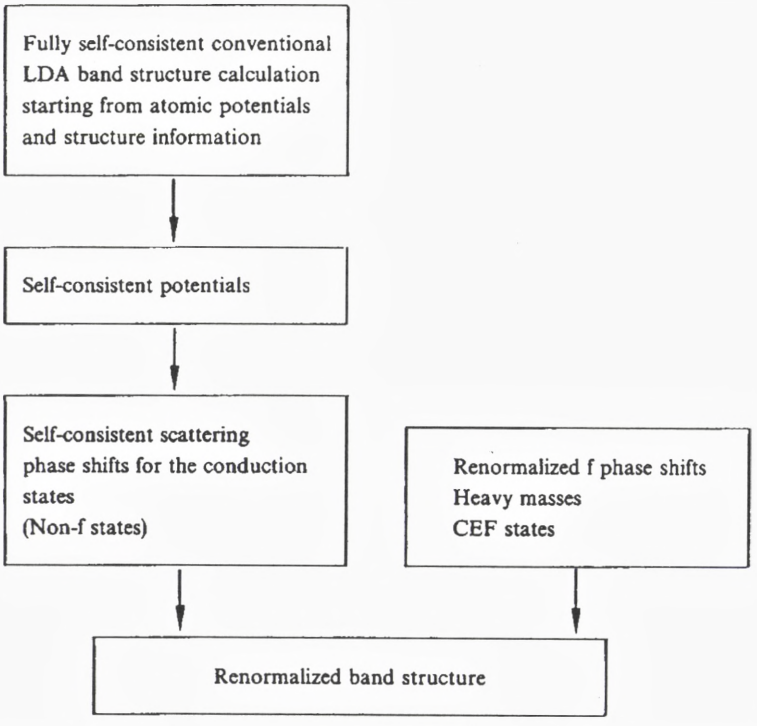

Figure 1. Different computational steps for a renormalized band-structure calculation (Zwicknagl, 1993)).

with $\epsilon_{\alpha=0} = 0$, $\epsilon_{\alpha=m} = \epsilon_{fm}$. The NCA equations have to be solved numerically (Bickers, 1987; Bickers et al., 1985). However, one can find simple, approximate solutions which have the virtue that crystal-field splittings can be explicitly included, a goal which has not been achieved yet by numerical methods. Once the $\rho_\alpha(\epsilon)$ are known, one can determine, e.g., the temperature dependence of the f-electron occupancies $n_{fm} = \langle f_m^+ f_m \rangle$ through

$$n_{fm}(T) = \frac{1}{Z_f} \int_{-\infty}^{+\infty} d\epsilon \, \rho_m(\epsilon) \, e^{-\beta(\epsilon-\mu)}, \tag{8}$$

where μ is the chemical potential and

$$Z_f = \int_C \frac{dz}{2\pi i} \, e^{-\beta z} \big(R_0(z) + \sum_m R_m(z)\big) \tag{9}$$

is the partition function of the f electrons. Knowing the $n_{fm}(T)$ enables us to compute quantities like the temperature dependence of the quadrupole moment of

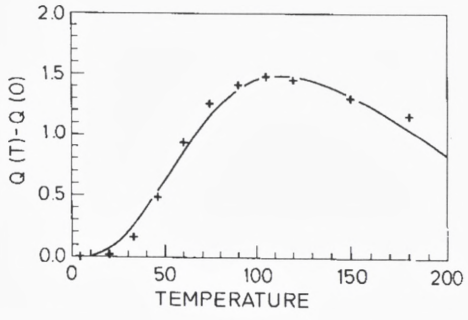

Figure 2. Temperature dependence of the quadrupole moment $Q(T)$ of the $4f$ electrons in $YbCu_2Si_2$. Crosses: experimental values; solid line: theoretical results for the parameters $T^* = 200$ K, $\Gamma = 47.4$ meV and a crystal-field parameter $3B_2^0 = -1.67$ meV (Zevin et al., 1988).

the f sites

$$Q(T) = \sum_m \langle m \mid (3J_z^2 - J^2) \mid m \rangle \, n_{fm}(T). \tag{10}$$

In Fig. 2 is shown a comparison between theory and experiments for the quadrupole moment of Yb in $YbCu_2Si_2$ (Thomala et al., 1990; Zevin et al., 1988). The input parameters are Γ, T^* and the CEF parameter B_2^0. The latter determines the crystal-field splitting of the $J = 7/2$ ground-state multiplet of Yb^{3+}.

When $T \gg T^*$, the f electrons can be treated as being localized. Their moment is weakly interacting with that of the conduction electrons and perturbation theory can be applied to study the resulting effects. The different temperature regimes are shown in Fig. 3. A beautiful demonstration of the above scenario is the experimentally observed difference in the Fermi surfaces of $CeRu_2Si_2$ and $CeRu_2Ge_2$ (King and Lonzarich, 1991). When Si is replaced by Ge the distance between Ce and its nearest neighbours is increased. This implies a decrease in the hybridization of the $4f$ electrons with the valence electrons of the neighbouring ions. While in $CeRu_2Si_2$ the characteristic temperature is $T^* \simeq 15$ K, it is practically zero in $CeRu_2Ge_2$. De

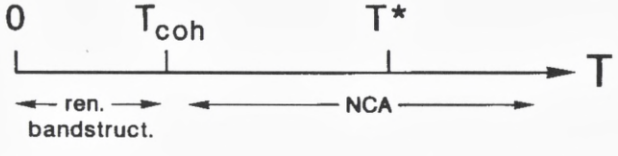

Figure 3. Different temperature regimes and theoretical methods for describing the low-energy excitations of a Kondo-lattice system

Haas–van Alphen experiments are performed at a temperature $T \simeq 1$ K implying $T \ll T^*$ for $CeRu_2Si_2$ while $T \gg T^*$ for $CeRu_2Ge_2$. Therefore, the $4f$ electron of Ce contributes to the volume of the Fermi sea in the former case, but not in the latter. Indeed, experiments show that the two Fermi surfaces have similar features but differ in volume by one electron (King and Lonzarich, 1991).

3 Zeeman route to heavy fermions

Low-temperature measurements of the specific heat and magnetic susceptibility demonstrate the existence of heavy-quasiparticle excitations in the electron-doped system $Nd_{2-x}Ce_xCuO_4$ (Brugger et al., 1993). For $x = 0.2$ and temperatures $T \leq 1$ K the linear specific heat coefficient is $\gamma = 4$ J/(mol K^2). The magnetic susceptibility χ_s is approximately T-independent in that temperature regime and the Sommerfeld–Wilson ratio is $R \simeq 1.8$ (see Fig. 4). While these features agree with those of other heavy-fermion systems, there are also pronounced differences. In superconducting heavy-fermion systems like $CeCu_2Si_2$ or UPt_3 the Cooper pairs are formed by the heavy quasiparticles. This is evidenced by the fact that the jump in the specific heat ΔC at the superconducting transition temperature T_c is directly related to the large γ coefficient, i.e., $\Delta C(T_c)/(\gamma T_c) \approx 2.4$. The low-energy excitations are therefore strongly reduced below T_c. In superconducting $Nd_{1.85}Ce_{0.15}CuO_4$ the formation of Cooper pairs has no noticeable effect on the heavy-fermion excitations. They remain unaffected by superconductivity.

A crucial difference between $Nd_{2-x}Ce_xCuO_4$ and, e.g., $CeCu_2Si_2$ are the strong electron correlations between the conduction electrons present in the former, but not in the latter material. In the two-dimensional Cu–O planes of $Nd_{2-x}Ce_xCuO_4$ with $x \geq 0.1$ we have to account for antiferromagnetic fluctuations which are very slow at low temperatures. There is considerable experimental evidence for this. Consider undoped Nd_2CuO_4, an antiferromagnet with a Néel temperature of $T_N \simeq 270$ K. Since the exchange interactions between a Nd ion and its nearest-neighbour Cu ions cancel because of the antiferromagnetic alignment of the Cu spins, one is left with the next-nearest neighbour Cu–Nd spin interaction. The latter is of the form $\alpha \mathbf{s}_{Cu} \cdot \mathbf{S}_{Nd}$ and is larger than the Nd–Nd interaction. The Schottky peak in the specific heat seen in Fig. 4 results from the spin flips of the Nd ions in the staggered effective field $\alpha \langle \mathbf{s}_{Cu} \rangle$ set up by the Cu spins (Zeeman effect). It is also present in doped systems like $Nd_{1.8}Ce_{0.2}CuO_4$ where antiferromagnetic long-range order is destroyed by doping. This can only be understood if the changes in the preferred direction of the Cu spins occur sufficiently slowly, i.e., slower than 10^{-10} s in the present case, so that the Nd spins can follow those motions adiabatically. Only then is a similar energy to that in Nd_2CuO_4 required to flip

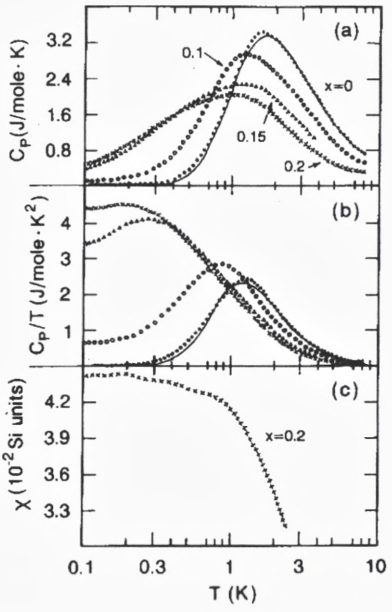

Figure 4. Heavy-fermion behaviour of $Nd_{2-x}Ce_xCuO_4$. (a) specific heat $C_p(T)$; (b) $C_p(T)/T$; (c) spin susceptibility for an overdoped sample with $x = 0.2$ (Brugger et al., 1993).

a Nd spin. This physical picture has been confirmed by recent inelastic neutron-scattering (Loewenhaupt et al., 1996) and μSR experiments (J. Litters, private communication). Spin-glass behaviour can be excluded.

Due to an effective valency of Ce of approximately +3.5 the Cu–O planes are doped with electrons, i.e., a corresponding number of Cu sites are in a $3d^{10}$ configuration. Since these sites have no spin they do not interact with the Nd ions. The extra electrons move freely in the Cu–O planes and therefore, the interaction of a Nd ion with the next-nearest Cu site is repeatedly turned off and on. It is this feature which results in heavy-quasiparticle excitations.

Two model descriptions have been advanced in order to explain the low-energy excitations of $Nd_{2-x}Ce_xCuO_4$. One is based on a Hamiltonian in which the Nd–Cu interaction is treated by a hybridization between the Nd $4f$ and Cu $3d$ orbitals. Usually it is much easier to extract heavy quasiparticles from such a Hamiltonian than from one with a spin–spin interaction obtained after a Schrieffer–Wolff transformation. The slow, antiferromagnetic fluctuations of the Cu spins are replaced by a static staggered field acting on them. This symmetry-breaking field also accounts for the strong correlations in the Cu–O planes because charge fluctuations between

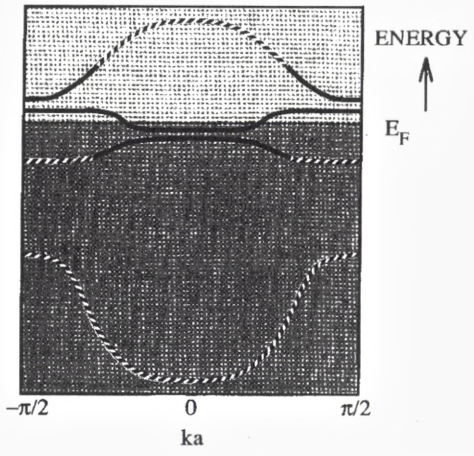

Figure 5. Schematic drawing of the quasiparticle excitation bands of $Nd_{2-x}Ce_xCuO_4$ for $x > 0$ (electron doping). The Fermi energy is indicated by a dotted line. Dashed lines: d-like excitations and solid lines: f-like excitations.

Cu sites are strongly reduced this way (unrestricted Hartree–Fock). Thus H reads

$$\begin{aligned} H &= -t \sum_{<ij>\sigma} (a^+_{i\sigma} a_{j\sigma} + \text{h.c.}) + h \sum_{i\sigma} \sigma e^{i\mathbf{Q}\cdot\mathbf{R}_i} a^+_{i\sigma} a_{i\sigma} \\ &+ V \sum_{i\sigma} (a^+_{i\sigma} f_{i\sigma} + \text{h.c.}) + \tilde{\epsilon}_f \sum_{i\sigma} f^+_{i\sigma} f_{i\sigma}. \end{aligned} \tag{11}$$

Here $\mathbf{Q} = (\pi, \pi)$ is a reciprocal lattice vector, $\mathbf{R}_i$ denotes the positions of the Cu ions and h is the size of the staggered field. The operators $a^+_{i\sigma}$, $f^+_{i\sigma}$ create an electron in the Cu $3d_{x^2-y^2}$ and the Nd $4f$ orbital, respectively. For simplicity, only one Nd site per Cu site is considered and one $4f$ orbital with energy $\tilde{\epsilon}_f$ is assumed instead of seven. The energies $\tilde{\epsilon}_f$ and V are strongly renormalized quantities because of the $4f$ electron correlations.

The Hamiltonian (11) is easily diagonalized. Four bands are obtained, two of which are d-like (Cu) and two which are f-like (Nd). The dispersions of the four bands are given by

$$E_\nu(\mathbf{k}) = \frac{\tilde{\epsilon}_f \pm \epsilon_\mathbf{k}}{2} \pm \frac{1}{2}\sqrt{(\epsilon_\mathbf{k} \mp \tilde{\epsilon}_f)^2 + 4V^2}\ , \ \nu = 1, \ldots, 4 \tag{12}$$

where $\epsilon_\mathbf{k} = (\epsilon_0^2(\mathbf{k}) + h^2/4)^{1/2}$ and $\epsilon_0(\mathbf{k}) = -2t(\cos k_x + \cos k_y)$. A schematic plot is shown in Fig. 5. At half-filling only the lower f band is filled and the Schottky-peak contributions to $C(T)$ are due to transitions from the filled lower to the empty

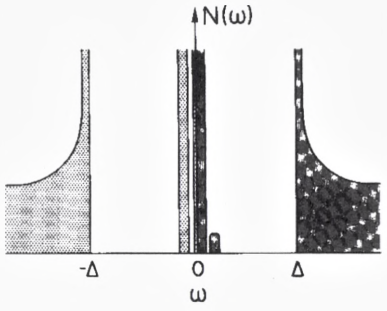

Figure 6. Superconducting density of states for $Nd_{1.85}Ce_{0.15}CuO_4$. A BCS-like model has been assumed. The f-like low-energy excitations remain virtually unchanged by the superconducting order parameter (Courtesy of G. Zwicknagl and S. Tornow).

upper f band. When the planes are doped with electrons the upper f band becomes partially filled resulting in low-energy excitations with large effective mass. The latter follows from the quasiparticle dispersion

$$E_{\rm qp}(\mathbf{k}) \simeq \tilde{\epsilon}_f + \frac{V^2}{(\tilde{\epsilon_f} + \epsilon_{\mathbf{k}})}. \tag{13}$$

It is noticed that here it is the Zeeman splitting of the f states which is responsible for the occurrence of heavy-electron behaviour. The effect of superconductivity on the heavy quasiparticles can be studied by adding an attractive interaction part $H_{\rm attr}$ for the charge carriers in the Cu–O planes to the Hamiltonian (Fulde and Zevin, 1993). For $V = 0$ the conventional BCS spectrum is recovered for the electrons in the upper Cu band. When $V \neq 0$ the lower Cu band hybridizes with one of the dispersionless f bands. The lower d band remains unaffected by superconductivity because pairing occurs in the upper d band. Therefore, superconductivity has no effect here. The upper d band hybridizes with the second f band. When H is diagonalized one finds a BCS gap in the Cu band while the f band remains virtually unchanged as compared with a vanishing superconducting order parameter. The resulting density of states is shown in Fig. 6. The structure inside the gap stems from the spin degrees of freedom of the Nd ions.

The second model description of the Nd spins coupled to the Cu spin is based on stochastic forces acting on the latter (Igarashi et al., 1995). They mimic the interaction of the Cu spin with its environment, i.e., with the other Cu spins. In that case we start from the Hamiltonian

$$H_{\rm int} = \alpha\, \mathbf{s}_{\rm Cu} \cdot \mathbf{S}_f\,, \qquad \alpha > 0 \tag{14}$$

for the Nd–Cu interaction. For simplicity, both spins are assumed to be of magnitude S. We treat the vector $\mathbf{\Omega} = \mathbf{s}_{\mathrm{Cu}}/S$ like a classical variable, subject to a stochastic force. We assume a Gauss–Markov process in which case the distribution function obeys a Fokker–Planck equation. The correlation function is then of the form

$$\langle \mathbf{\Omega}(0)\mathbf{\Omega}(t)\rangle = e^{-2D_r t} \tag{15}$$

where D_r can be obtained from the nonlinear σ model (Chakravarty et al., 1989; Chakravarty and Orbach, 1990). Because there is no long range-order $\langle \mathbf{\Omega}(0)\rangle = \mathbf{0}$. The motion of the Nd spin is governed by the equation

$$\frac{d}{dt}\,\mathbf{n}(t) = \omega_0\big(\mathbf{\Omega}(t) \times \mathbf{n}(t)\big) \tag{16}$$

where $\mathbf{n}(t) = \mathbf{S}_f/S$ and $\omega_0 = \alpha S$. The spectral function

$$I(\omega) = \frac{1}{2\pi}\int_{-\infty}^{+\infty} dt\, e^{i\omega t}\langle \mathbf{n}(0)\mathbf{n}(t)\rangle \tag{17}$$

is evaluated by making use of the corresponding stochastic Liouville equation. We find that $I(\omega)$ is of the form

$$I(\omega) = \frac{1}{3\pi}\,\frac{4D_r}{\omega^2 + (4D_r)^2} \;+ (\text{side peaks at } \omega_0). \tag{18}$$

While $D_r(T)$ vanishes as $T \to 0$ in the presence of long-range order, it remains finite when the latter is destroyed by doping. A linear specific heat contribution of the $4f$ spin is obtained from

$$C(T)_{\mathrm{imp}} = \frac{d}{dT}\langle H_{\mathrm{int}}\rangle = \frac{S(S+1)}{T^2}\int_0^{\infty} d\omega\,\omega^2\,\frac{I(\omega)}{\cosh^2(\omega/2T)} \tag{19}$$

when $D_r(T = 0) \neq 0$. The side peaks in $I(\omega)$ give raise to a Schottky-type contribution. The calculated specific heat is shown in Fig. 7 and reproduces the experiments reasonable well (compare with Fig. 4). One shortcoming of the theory in its present form is the low-temperature spin susceptibility which follows from

$$\chi_{\mathrm{imp}}(T) = \frac{4}{3}(g\mu_B)^2 S(S+1)\int_0^{\infty} d\omega\,\frac{I(\omega)}{\omega}\tanh\frac{\omega}{2T}. \tag{20}$$

We find $\chi_{\mathrm{imp}}(T) \sim \ln(D_r/T)$ at low T. This is possibly due to the neglect of Nd–Nd interactions. However, when evaluated for $T = 0.4$ K one finds for $Nd_{1.8}Ce_{0.2}CuO_4$ a Sommerfeld–Wilson ratio of $R \simeq 1.4$.

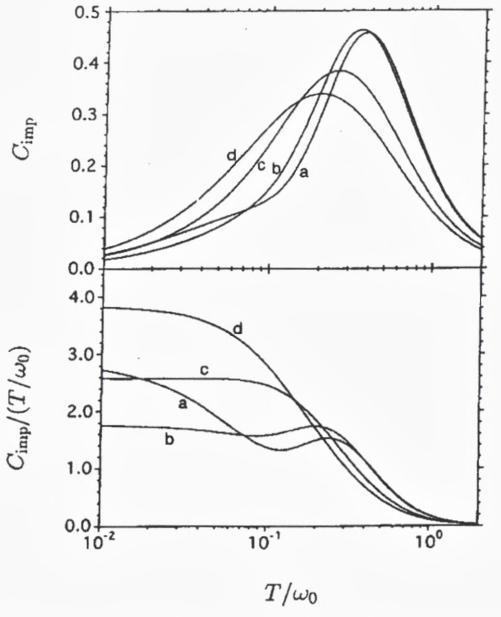

Figure 7. Specific heat contribution of a Nd ion with $S = 1/2$. Curves (a)-(d) correspond to $D_\tau/\omega_0 = 0.05, 0.1, 0.5, 0.8$, respectively (Igarashi et al., 1995).

4 Hubbard chains - Yb_4As_3

The intermetallic compound Yb_4As_3 is of the anti-Th_3P_4 structure. The Yb ions are situated on chains with directions along the diagonals of a cube. Thus we are dealing with a system of four sets of interpenetrating chains (see Fig. 8). We want to draw attention to the fact that the distance between neighbouring Yb ions on a chain exceeds the one between neighbouring ions on different chains.

Because As has a valency of -3, three of the four Yb ions have a filled $4f$ shell, i.e., a valency $+2$, while one ion is in a $4f^{13}$ configuration (valency $+3$). Since all Yb sites are equivalent, the hole in the $4f$ shell is shared between four Yb ions and the system is metallic. However, at a temperature $T_s \simeq 300$ K the system undergoes a weak first-order phase transition into a trigonal distorted structure (Ochiai et al., 1990; Suzuki, 1993; Ochiai et al., 1993; Reinders et al., 1993; Kasuya, 1994; Bonville, 1994). Thereby one set of chains, e.g., along $[1, 1, 1]$ is shortened while the other three sets are elongating thereby leaving the volume of the unit cell unchanged. This results in charge ordering because the Yb^{3+} ions have a smaller ionic radius than the Yb^{2+} ones and occupy the chains with smaller Yb–Yb distances (short chains) (Kasuya, 1994). The driving force for the phase transition

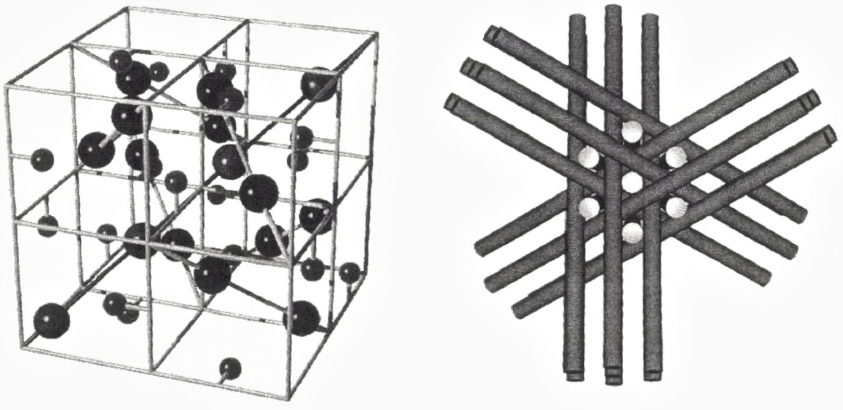

Figure 8. (a) Structure of Yb_4As_3: large and small spheres represent the Yb and As ions, respectively. (b) Four sets of interpenetrating chains on which the Yb ions are located.

is the Coulomb repulsion between Yb^{3+} ions. Measurements of the Hall constant reveal a dramatic increase below T_s, implying a sharp drop in the charge carrier density with decreasing temperature. At low T one is left with one carrier per 10^3 Yb ions. The resistivity increases below T_s with decreasing temperature until it reaches a maximum of approximately 10 mΩ cm. At low T it is of the form $\rho(T) = \rho_0 + AT^2$ and therefore shows Fermi-liquid behaviour. The linear specific-heat coefficient γ is found to be of order $\gamma \simeq 200$ mJ/(mol K^2). The spin susceptibility is Pauli like and equally enhanced as γ, giving raise to a Sommerfeld–Wilson ratio of order unity. No indication of magnetic order is found down to $T = 0.045$ K, but below 2 K the susceptibility increases again which indicates the presence of another low energy scale (Bonville et al., 1994). The above findings strongly suggest heavy-fermion behaviour which is further confirmed by the observation that the ratio A/γ^ν ($\nu \simeq 2$) compares well with that of other heavy-fermion systems (Ochiai et al., 1993). One should appreciate that despite the low-carrier concentration the γ value exceeds that of, e.g., Na by a factor of more than 10^2. This demonstrates that the high density of low-energy excitations must clearly involve spin-degrees of freedom of the Yb^{3+} ions. The Kondo effect can be ruled out as a source of heavy quasiparticles. The low-energy scale which corresponds to the observed γ value is $T^* \simeq 40$ K. But inelastic neutron scattering shows a well resolved crystal-field excitation of Yb^{3+} at a comparable energy which would be impossible if local singlets would form with a binding energy of similar size.

A theory has been developed which can explain rather consistently the above

experimental findings. It is based on interpreting the structural phase transition in terms of a collective band Jahn–Teller (CBJT) effect (Fulde et al., 1995). The transition is caused by a strong deformation-potential coupling which is quite common in mixed-valence systems. It is based on the Coulomb repulsion between different rare-earth ions. The CBJT transition splits the fourfold degenerate quasi-1d density of states into a nondegenerate one corresponding to the short chains and a threefold one due to the long chains. The nondegenerate one is lower in energy and would be half filled if charge ordering were perfect and the holes were uncorrelated fermions. Instead, the holes are strongly correlated. Two holes on a site imply a $4f^{12}$ configuration for Yb and that has a much too high energy to occur. Therefore, we are dealing with an almost full lower (hole) Hubbard band rather than with an almost half-filled band. Therefore, the ideal system should be an insulator. That Yb_4As_3 is a semimetal and not an insulator is probably related to the nonvanishing hopping matrix elements between $4f$ orbitals in the long and short chains. This may result in self-doping with a fraction of holes moving from the short to the long chains. Accurate conditions for self-doping are not easily worked out, but a first step in this direction was recently done (Blawid et al., 1996).

The phase transition can be described by an effective Hamiltonian of the form

$$H = -t \sum_{\mu=1}^{4} \sum_{<ij>\sigma} (f^{+}_{i\mu\sigma} f_{j\mu\sigma} + \text{h.c.}) + \epsilon_\Gamma \sum_{i,\mu=1}^{4} \Delta_\mu f^{+}_{i\mu\sigma} f_{i\mu\sigma} + 4N_L c_0 \epsilon_\Gamma^2. \tag{21}$$

The operators $f^{+}_{i\mu\sigma}(f_{i\mu\sigma})$ create (destroy) a $4f$ hole at site i of chain μ with effective spin σ (the crystal-field ground state of the $J = 7/2$ multiplet is two-fold degenerate). Interchain hopping matrix elements are neglected and so is the on-site Coulomb repulsion between holes, since near T_s holes are reasonably well separated. The notation $<ij>$ refers to Yb–Yb nearest neighbours in a chain of length N_L. The trigonal-strain order parameter $\epsilon_\Gamma < 0$ corresponds to the bulk elastic constant $4c_0$. The deformation potential Δ_μ is

$$\Delta_\mu = \Delta \begin{cases} 1 & \mu = 1 \\ -\frac{1}{3} & \mu = 2, 3, 4. \end{cases} \tag{22}$$

With a choice of $4t = 0.2$ eV obtained from LDA calculations, $c_0 = 10^{11}\ \Omega\,\text{erg/cm}^3$ (Ω is the volume of a unit cell) and $\Delta = 5$ eV we obtain $T_s \simeq 250$ K.

With increasing charge ordering (see Fig. 9), correlations become more and more important because with the increase in concentration of holes in the short chains their average distance decreases. Therefore, at low temperatures T the t–J Hamiltonian or a Hubbard Hamiltonian must be used. Using the former and making use of a slave-boson mean-field approximation we arrive at an effective

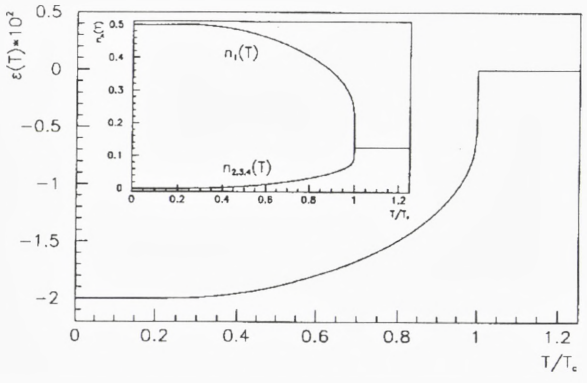

Figure 9. Temperature dependence of the trigonal-strain order parameter $\epsilon_\Gamma(T)$. Shown as an inset are the occupation numbers n_μ of the short ($\mu = 1$) and long ($\mu > 1$) chains (Bonville et al., 1994).

mass enhancement of the form

$$\frac{m^*}{m_b} = \frac{t}{t\delta + (3/4)\,\chi J}. \tag{23}$$

Here m_b denotes the band mass, $\chi = \chi_{ij} = \langle \sum_\sigma f^+_{i1\sigma} f_{j1\sigma} \rangle$, δ is the deviation of the short chains denoted by 1 from half filling and $J = 4t^2/U$, where U is the on-site Coulomb repulsion between holes. With $U = 10$ eV one finds $J = 10^{-3}$ eV and using $\chi(T = 0) = (2/\pi)\sin(\pi(1 - \delta)/2)$ with $\delta = 10^{-3}$ one obtains a ratio of $m^*/m_b \simeq 100$. This derivation of the mass enhancement hides somewhat the fact that spin degrees of freedom are responsible for the heavy quasiparticles. A more direct way of understanding the large γ value in the specific heat is by realizing that a spin chain gives rise to a linear specific heat. Although a Heisenberg chain has no long-range order, short-range antiferromagnetic correlations lead to spin-wave like excitations which can be rather well described by linear spin-wave theory. Indeed, Kohgi et al. (private communication) measured the spin-excitation spectrum by inelastic neutron scattering and found a one-dimensional spin-wave spectrum.

Since spin-wave-like excitations are responsible for the fermionic low-energy excitations associated with the specific heat and susceptibility we are dealing here with charge-neutral heavy fermions in distinction to the charged heavy electrons, which appear, e.g., in $CeAl_3$. Therefore, we speak of an uncharged or neutral heavy Fermi liquid.

The physical interpretation given above allows for an explanation of another experiment. It has been previously found that an applied magnetic field of 4 tesla has little influence on the γ coefficient above 2 K, but suppresses γ considerably below

2 K (Helferich, Steglich and Ochiai, private communication). This effect is unexpected, since one would have thought that the changes are of order $(\mu_B H/k_B T^*)^2$ and therefore very small. However, we can explain the experiments by providing for a weak coupling between parallel short chains. When linear spin-wave theory is applied, a ratio between interchain and intrachain coupling of order 10^{-4} opens an anisotropy gap which modifies $C(T)$ in accordance with observation (Schmidt et al., 1996).

5 Conclusions

We have shown that heavy-fermion excitations may be of very different physical origin. Three distinct mechanisms have been discussed which result in low-energy scales required for the heavy quasiparticles. The most, and until recently only one studied so far refers to Kondo lattices and is based on the formation of (local) singlet states. They result from a weak hybridization of the $4f$ electrons with the conduction electrons. In that case the low-energy scale is given by the binding energy associated with the singlets. In distinction to Kondo lattices we are dealing in the case of $Nd_{2-x}Ce_xCuO_4$ with a lattice of Nd ions with a well localized magnetic moment which are coupled to a two-dimensional system of strongly correlated conduction electrons. In that case a low-energy scale is provided by the Zeeman energy of the Nd magnetic moment in the slowly fluctuating molecular field set up by the Cu spins. Finally, in Yb_4As_3 the low-energy scale is due to the band width of the spin-wave like excitations in magnetic chains formed by Yb^{3+} ions. The few carriers, i.e., one per 10^3 Yb ions are unimportant for the low temperature specific heat which is governed exclusively by spin excitations (spinons). The system serves as an example of almost perfect separation between spin and charge degrees of freedom. For the purpose of understanding its low temperature thermodynamic properties it can be considered a neutral or chargeless heavy Fermi liquid. Yb_4As_3 belongs to a class of materials often referred to as low-carrier Kondo systems or Kondo insulators (for recent references see, e.g., Proc., 1996). As we have shown that might be misleading, at least for Yb_4As_3, where the appearance of heavy fermions has nothing to do with the Kondo effect. However, that material is rather distinct to CeNiSn or other members of that class. Therefore, the origin of low-energy scales must be investigated from case to case.

In summary, heavy-fermions behaviour can have a variety of physical origins. It remains a challenge for the future to uncover other processes leading to low-energy scales.

Acknowledgements

I would like to acknowledge very fruitful and stimulating collaborations with Drs. J. Igarashi, K. Murayama, B. Schmidt, P. Thalmeier, V. Zevin and G. Zwicknagl.

References

Aoki H, Uji S, Albessand A and Onuki Y, 1993: Phys. Rev. Lett. **71**, 2120
Bickers NE, 1987: Rev. Mod. Phys. **59**, 845
Bickers NE, Cox DL and Wilkins J.W, 1985: Phys. Rev. Lett. **54**, 230
Blawid S, Hoang AT and Fulde P, 1996: Phys. Rev. B (in print)
Bonville P, Ochiai A, Suzuki T and Vincent E, 1994: J. Phys. I **4**, 595
Brugger T, Schreiner T, Roth G, Adelmann P and Czjzek G. 1993: Phys. Rev. Lett. **71**, 2481
Chakravarty S and Orbach R, 1990: Phys. Rev. Lett. **64**, 224
Chakravarty S, Halperin BI, Nelson DR, 1989: Phys. Rev. B **39**, 2344
d'Ambrumenil N and Fulde P, 1985: J. Magn. Magn. Mater. **47–48**, 1
Doniach S, 1971: Physica B **91**, 231
Doniach S, 1987: *Theoretical and Experimental Aspects of Valence Fluctuations and Heavy Fermions*, eds. L.C. Gupta and S.K. Malik (Plenum Press, New York 1987) p. 179
Fulde P and Jensen J, 1983: Phys. Rev. B **27**, 4085
Fulde P and Zevin V, 1993: Europhys. Lett. **24**, 791
Fulde P, Keller J and Zwicknagl G, 1988: *Solid State Physics*, eds. H. Ehrenreich and D. Turnbull (Academic Press, San Diego) Vol. 41, p. 1
Fulde P, Schmidt B and Thalmeier P, 1995: Europhys. Lett. **31**, 323
Fulde P, Zevin V and Zwicknagl G, 1993: Z. Phys. B **92**, 133
Grewe N and Steglich F, 1991: *Handbook on the Physics and Chemistry of Rare Earths*, eds. K.A. Gschneidner, Jr. and L. Eyring (North-Holland, Amsterdam) Vol. 14
Hewson AC, 1993: *The Kondo Problem to Heavy Fermions* (Cambridge University Press, Cambridge)
Igarashi I, Murayama K and Fulde P, 1995: Phys. Rev. B **52**, 15966
Kasuya T, 1993: *Transport and Thermal Properties of f-Electron Systems*, eds. G. Oomi et al. (Plenum Press, New York)
Kasuya T, 1994: J. Phys. Soc. Jpn. **63**, 2481
Keiter H and Kimball JC, 1971: Int. J. Magn. **1**, 233
King C.A and Lonzarich GG, 1991: Physica B **171**, 161
Kojima H, Kuramoto Y and Tachiki M, 1984: Z. Phys. B **54**, 293
Lee PA, Rice TM, Serene JM, Sham LJ and Wilkins JW, 1986: Comments Condens. Matter Phys. **12**, 99
Loewenhaupt M, Metz A, Pyka NM, McK Paul DM, Martin J, Duijn VHM, Franse JJM, Mutka H and Schmidt W, 1996: Ann. Phys. **5**, 197
Lonzarich GG, 1988: J. Magn. Magn. Mater. **76–77**, 1
Norman M.N, Koelling D, 1993: *Handbook on the Physics and Chemistry of Rare Earths*, eds. K.A. Gschneidner, L. Eyring, G.H. Lander and G.R. Choppin (Elsevier, Amsterdam) Vol. 17, p. 1
Ochiai A, Li DX, Haga Y, Nakamura O and Suzuki T, 1993: Physica B **186–188**, 437
Ochiai A, Suzuki T and Kasuya T, 1990: J. Phys. Soc. Jpn. **59**, 4129
Ott HR, 1987: Prog. Low Temp. Phys. **11**, 215
Proc. of the Inter. Conf. on Strongly Correlated Electron Systems, 1995: Physica B **206–207**

Proc. of the Inter. Conf. on Strongly Correlated Electron Systems, 1996: Physica B **223–224**
Razafimandimby H, Fulde P and Keller J, 1984: Z. Phys. B **54**, 111
Reinders PHP, Ahlheim U, Fraas K, Steglich F and Suzuki T, 1993: Physica B **186–188**, 434
Schlottmann P, 1984: Phys. Rep. **181**, 1
Schmidt, B, Thalmeier P and Fulde P, 1996: Europhys. Lett. **35**, 109
Stewart GR, 1984: Prog. Low Temp. Phys. **56**, 755
Sticht J, d'Ambrumenil N and Kübler 1986: J, Z. Phys. B **65**, 149
Strange P and Newns DM, 1986: J. Phys. F **16**, 335
Suzuki T, 1993: Physica B **186–188**, 347
Thomala K, Weschenfelder G, Czjzek G and Holland-Moritz E, 1990: J. Magn. Magn. Mater. **89**, 143
Varma CM and Yafet Y, 1976: Phys. Rev. B **13**, 2950
Wachter P, 1994: *Handbook on the Physics and Chemistry of Rare Earths*, eds. K. A. Gschneidner, Jr., L. Eyring, G. H. Lander and G.R. Chappin (Elsevier, Amsterdam) Vol. 19
White RM and Fulde P, 1981: Phys. Rev. Lett. **47**, 1540
Yoshida K, 1966: Phys. Rev. **147**, 223
Yoshida K and Yoshimori A, 1973: *Magnetism*, eds. G.T. Rado and H. Suhl (Academic Press, New York) Vol. 5, p. 253
Zevin V, Zwicknagl G and Fulde P, 1988: Phys. Rev. Lett. **60**, 2331
Zwicknagl G, 1988: J. Magn. Magn. Mater. **76–77**, 16
Zwicknagl G, 1993: Adv. Phys. **41**, 203
Zwicknagl G, Runge E and Christensen NE, 1990: Physica B **163**, 97